Analytical Model for the Rectangular Power-Ground Structure Including Radiation Loss

Richard L. Chen, *Member, IEEE*, Ji Chen, *Member, IEEE*, Todd H. Hubing, *Senior Member, IEEE*, and Weimin Shi, *Senior Member, IEEE*

***Abstract*—An accurate analytical model to predict via coupling within rectangular power-return plane structures is developed. Loss mechanisms, including radiation loss, dielectric loss, and conductor loss, are considered in this model. The radiation loss is incorporated into a complex propagating wavenumber as an artificial loss mechanism. The quality factors associated with three loss mechanisms are calculated and compared. The effects of radiation loss on input impedances and reflection coefficients are investigated for both high-dielectric-loss and low-dielectric-loss printed circuit boards. Measurements are performed to validate the effectiveness of this model.**

***Index Terms*—Power and ground-plane noise, quality factor, radiation loss, via coupling.**

I. Introduction

POWER and ground-plane noise, also known as simultaneous switching noise (SSN), inductive noise or Delta-I noise, can appear in printed circuit board (PCB) and multichip module (MCM) designs when a high-speed time-varying or a transient current flows through a via [1]–[5]. Due to the via discontinuity, part of the power is transmitted into the substrate and coupled to other devices on the PCB. The signal coupled to other devices may cause signal integrity and electromagnetic compatibility (EMC) issues [1]–[5]. As the clock frequency increases and the rise time decreases, the likelihood of significant mutual coupling occurring between a via and its neighboring devices increases. The signal can also radiate into its environment and cause electromagnetic interference (EMI) problems [6]. Therefore, to ensure successful designs of high-speed electronic products, it is important to develop modeling techniques that can accurately estimate the mutual coupling between a via and its surrounding devices and predict the PCB radiation due to via discontinuities.

Power-return plane modeling has been carried out by using analytical methods [1]–[3] and full-wave techniques [4], [5], [7]. The analytical methods use either the radial waveguide model or the cavity model to extract the structure's input impedance or mutual impedance. The computational cost of analytical approaches is typically much less than that of the full-wave techniques and the underlying physical mechanism is also clearer. Therefore, an analytical approach is preferred whenever it is possible. However, to our knowledge, existing analytical approaches ignore radiation loss in the input impedance or mutual impedance estimation. This approximation may lead to significant errors in the input impedance estimation for some PCB structures. In [6], the radiated field of a rectangular power-return plane structure was investigated as an electromagnetic interference problem, a strong radiation effect is observed at resonant frequencies. However, the effect of the radiation on the via input impedance or the mutual impedance were not studied. In [8], radiation effects on the input impedance were investigated for a circular PCB structure. In the model, the radiation loss is considered by introducing a nonzero surface admittance around the cavity and is calculated using the spectral domain immittance (SDI) approach [9]. The results showed that the radiation loss cannot be neglected at the resonant frequencies, particularly for thick substrate PCBs. Unfortunately, this approach is not directly applicable to the via discontinuity analysis for general power-return plane structures since the constant edge impedance assumption is not valid for practical rectangular structures.

The purpose of this paper is to introduce a more general approach to include the radiation loss in analyzing practical rectangular power-return plane structures. Rather than calculating the location- and mode-dependent edge impedance on the periphery of the power-return plane [10], the effect of the radiation loss is accounted for by assuming an equivalent loss in the complex propagating wavenumber. The radiation loss is calculated by integrating the radiation fields of equivalent magnetic currents on the edges of the PCBs.

The remainder of the paper is organized as follows. Section II describes the development of the input impedance model and mutual impedance that include dielectric loss, conductive loss, and radiation loss. The procedure for calculating the radiation loss quality factor is described in Section III. In Section IV, the approach is applied to analyze the input impedance, reflection coefficients and mutual impedance of two typical power-return plane structures and results are compared with experimental data. Conclusions are given in Section V.

II. Input Impedance Model

A typical rectangular power-return plane structure is shown in Fig. 1. It consists of two metal plates with length, l, and width,

Manuscript received January 13, 2004; revised July 3, 2004. This work was supported by the Texas Higher Education Coordinating Board under Grant 003652-0195-2001.

R. L. Chen and J. Chen are with the Department of Electrical and Computer Engineering, University of Houston, Houston, TX 77204 USA (e-mail: jchen18@ uh.edu).

T. H. Hubing is with the Department of Electrical and Computer Engineering, University of Missourri, Rolla, MO 55409 USA.

W. Shi is with the Desktop Platform Group, Intel Corporation, Hillsboro, OR 97124 USA.

Digital Object Identifier 10.1109/TEMC.2004.842204

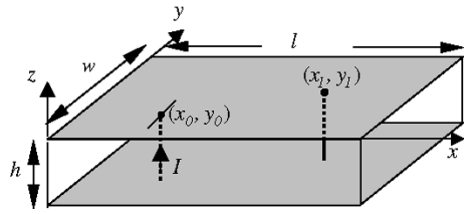

Fig. 1. A rectangular power-return plane structure.

w, and a dielectric slab (with a thickness of h) sandwiched between the two metal plates. The metal plates have a conductivity of σ and the substrate has a relative dielectric constant of ϵ_r and a loss tangent of $\tan\delta$. A via with a radius of r_0 is located at (x_0, y_0) and a current source I is impressed into the via. Another via locates at (x_1, y_1) for mutual coupling consideration.

The power-return plane can be approximated by a cavity model where the top and bottom walls are perfect electric conductor (PEC) walls and the four side walls are perfect magnetic conductor (PMC) walls [11]. Since the substrate is electrically thin, only the transverse magnetic (TM) modes need to be considered [11]. To account for the fringing effects, an effective length, $l_e = l + (h/2)$ and an effective width, $w_e = w + (h/2)$, are used. This simplified model, however might introduce a slight resonant frequency deviation, especially at the high-frequency end, as we will show in Section IV. Furthermore, the edge extension is closely related to the stored energy and it is also mode dependent. Hence, the simplified model can also introduce small errors on radiation loss calculation. More accurate empirical models for the effective length/width are available in [12], [13], but they are derived for the dominant mode and assumed to work for other modes. Therefore, the simplified effective length–width model is used in this study.

The electric field in the rectangular cavity can be written as [11]

$$E_z(x,y) = \sum_{m=0}^{\infty}\sum_{n=0}^{\infty} A_{mn}\psi_{mn}(x,y) \tag{1}$$

where

$$\psi_{mn}(x,y) = \cos\left(\frac{m\pi x}{l_e}\right)\cos\left(\frac{n\pi y}{w_e}\right) \tag{2}$$

represents a cavity mode ($\mathrm{TM_{mn}}$) supported by the structure. The corresponding excitation coefficient is determined by the inner product of the mode and the source, shown as

$$A_{mn}(x,y) = \frac{j\omega\mu\langle J_z,\ \psi_{mn}\rangle}{\langle\psi_{mn},\ \psi_{mn}\rangle}\frac{1}{k_{1e}^2 - k_{mn}^2} \tag{3}$$

where J_z is the driving current density,

$$k_{mn} = \sqrt{(m\pi/l_e)^2 + (n\pi/w_e)^2}$$

and k_{1e} is the effective wave number given by [14]

$$k_{1e} = k_1\sqrt{1 - jL_s}. \tag{4}$$

In (4), $k_1 = \omega\sqrt{\mu\varepsilon_r\varepsilon_0}$ and L_s is the total loss factor due to three loss mechanisms, including the conductor loss, the dielectric loss, and the radiation loss. It is given by [14]

$$L_s = \frac{1}{Q} = L_c + L_d + L_r \tag{5}$$

where Q stands for the total quality factor and L_c, L_d, and L_r represent the conductor loss, the dielectric loss and the radiation loss. The three loss factors can be written as

$$L_c = \frac{1}{Q_c} \tag{6}$$

$$L_d = \frac{1}{Q_d} \tag{7}$$

and

$$L_r = \frac{1}{Q_r} \tag{8}$$

where Q_c, Q_d, and Q_r represent quality factors of the conductor loss, the dielectric loss, and the radiation loss. The conductor and dielectric loss quality factors can be obtained as

$$Q_d = \frac{1}{\tan\delta} \tag{9}$$

and

$$Q_c = \frac{h}{\delta_s} \tag{10}$$

where δ_s is the skin depth, given as

$$\delta_s = \sqrt{\frac{2}{\omega\mu\sigma}}. \tag{11}$$

Assuming the total loss factor, $L_s \ll 1$, which is true for most of the substrate due to the narrow-band nature of power-return plane structures, applying the binomial expansion yields

$$k_{1e} = k_1\left(1 - j\frac{\tan\delta + \frac{\delta_s}{h}}{2} - j\frac{1}{2Q_r}\right). \tag{12}$$

As shown in the above equation, the three loss mechanisms are represented by the imaginary parts in the complex wavenumber. Neglecting the radiation loss ($Q_r = \infty$) yields the complex wavenumber given in [1], [15], which is valid when the dielectric loss or the conductor loss is dominant. However, when the substrate is thick or low loss, the assumption is no longer valid and the radiation loss has to be taken into consideration.

The impressed current on the via can be equivalently represented by an one-dimensional current (strip current) or a two-dimensional current (rectangular current) [1], [16]. In the one-dimensional current modeling, the via current is approximated using a strip current with a width of w_s, where $w_s = e^{3/2}r_0$ [16]. In the two-dimensional current modeling, the via current is approximated using a square current with a side width a_{square} of $\sqrt{\pi}r_o$ [1]. Both models are valid if the via size is much smaller

than that of the board size. For simplicity, we use the strip current approximation in this study. Using this model, the driving current density can be obtained by

$$J_z = \frac{I}{w_s}. \tag{13}$$

Substituting (12) and (13) into (3) and then substituting (3) into (1), one can obtain the input impedance as

$$\begin{aligned} Z_{in} &= -\frac{E_z h}{I} \\ &= \frac{-j\omega\mu h}{I^2} \sum_{m=0}^{\infty}\sum_{n=0}^{\infty} \frac{\langle J_z, \psi_{mn}\rangle^2}{\langle \psi_{mn}, \psi_{mn}\rangle} \frac{1}{k_{1e}^2 - k_{mn}^2} \end{aligned} \tag{14}$$

where

$$\langle J_z, \psi_{mn}\rangle = I \operatorname{sinc}\left(\frac{n\pi w_s}{2w_e}\right) \cos\left(\frac{m\pi x_0}{l_e}\right) \cos\left(\frac{n\pi y_0}{w_e}\right) \tag{15}$$

and

$$\langle \psi_{mn}, \psi_{mn}\rangle = \frac{w_e l_e}{4}(1+\delta_{m0})(1+\delta_{n0}). \tag{16}$$

In (13), δ_{n0} is defined as

$$\delta_{n0} = \begin{cases} 1, & \text{for } n = 0 \\ 0, & \text{for } n \neq 0. \end{cases}$$

Substituting (9) into (6) and also (10) into (7), one can obtain the dielectric loss factor and conductor loss factor directly. However, the radiation loss factor, L_r still needs to be evaluated numerically. In the next section, the steps to calculate the radiation quality factor Q_r are described.

Similar to [17], the mutual impedance between the via at (x_0, y_0) and the other via at (x_1, y_1) can be obtained as an integration of Green's function of the Helmholtz equation which satisfies the second kind boundary condition, shown as

$$\begin{aligned} Z_{\text{mutual}} = &-j\omega\mu h \sum_{m=0}^{\infty}\sum_{n=0}^{\infty} \frac{\operatorname{sinc}^2\left(\frac{n\pi w_s}{2w_e}\right)}{\langle \psi_{mn}, \psi_{mn}\rangle (k_{1e}^2 - k_{mn}^2)} \\ &\bullet \cos\left(\frac{m\pi x_0}{l_e}\right)\cos\left(\frac{m\pi x_1}{l_e}\right)\cos\left(\frac{n\pi y_0}{w_e}\right)\cos\left(\frac{n\pi y_1}{w_e}\right). \end{aligned} \tag{17}$$

III. Evaluation of Quality Factor for Radiation Loss

The radiation loss quality factor Q_r in (8) can be determined by using [18],

$$Q_r = \omega\left(\frac{U_s}{P_r}\right) \tag{18}$$

where U_s is the electromagnetic energy stored inside the cavity and P_r is the power radiated from the cavity. The radiation loss quality factor only needs to be evaluated at the power-return plane's resonant frequencies since the electric field in low loss cavities is much stronger at these frequencies than that at the off-resonance frequencies, as indicated in (3). With the low-loss assumption, at the resonant frequency f_{mn}, the total electric field can be approximated by the resonant mode TM_{mn} as [6]

$$E_z(x,y) \approx A_{mn} \cos\left(\frac{m\pi x}{l_e}\right) \cos\left(\frac{n\pi y}{w_e}\right). \tag{19}$$

With this electric field distribution, the stored energy is obtained by [18]

$$\begin{aligned} U_s &= 2U_E = 2\iiint_V \frac{1}{4}\varepsilon_0\varepsilon_r |E_z|^2 dV \\ &= \frac{1}{8}\varepsilon_0\varepsilon_r h |A_{mn}|^2 (1+\delta_{m0})(1+\delta_{n0}) \end{aligned} \tag{20}$$

and the radiated power can be obtained by [19]

$$P_r = \int_0^{2\pi}\int_0^{\pi} S_r(r,\theta,\varphi) r^2 \sin\theta d\theta d\varphi \tag{21}$$

where

$$S_r(r,\theta,\varphi) = \frac{1}{2\eta_0}\left[|E_\theta|^2 + |E_\varphi|^2\right] \tag{22}$$

is the magnitude of Poynting vector. The transverse spherical electric far-field components E_θ and E_φ can be calculated by the analytical solutions given in the Appendix, as developed in [6] by integration over the equivalent magnetic currents along the edges of the parallel plates. Due to the complexity of the analytical field expression for E_θ and E_φ, the integration in (22) has to be performed numerically. Once the U_s and P_r are obtained, the effect of radiation loss on the input impedance can be evaluated by (18).

IV. Numerical and Experimental Results

In this section, the developed modeling technique is applied to two typical power-return plane structures. The section starts with an investigation and comparison of the three types of loss mechanisms. Then, the input impedance, reflection coefficient, or mutual impedance is calculated and also validated by experimental results.

A. Three Loss Mechanisms

To investigate the importance of radiation effects on input impedance, the radiation loss factor, L_r needs to be compared with the other two loss factors, L_c and L_d. The first example considered here is a FR4 test board with a dimension of $16 \times 10 \times 0.127$ cm^3. The substrate has a relative dielectric constant of 3.84 and a loss tangent of 0.019. The board is fed by an SMA connector (with an inner radius of 6.25×10^{-2} cm) at the location $x_0 = 4.0$ cm and $y_0 = 5.0$ cm. The conductivity of copper used for the calculations was 5.813×10^7 S/m. The loss factors for all three loss mechanisms are shown in Fig. 2. For this board, the dominant loss is the dielectric loss ($L_d = 0.019$), which is assumed to be a constant over the entire frequency range.

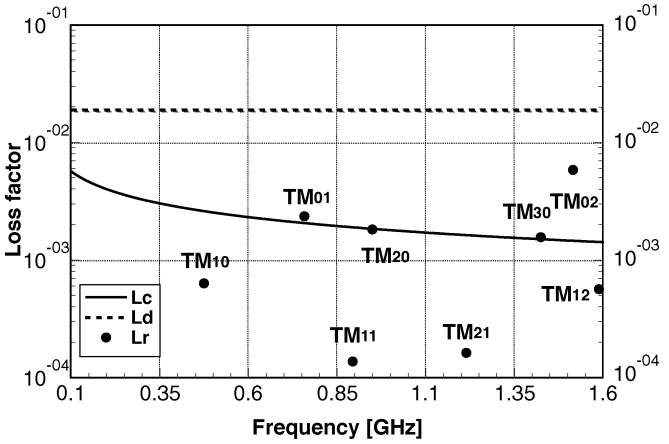

Fig. 2. Calculated loss factors for a $16 \times 10 \times 0.127$ cm^3 power-ground plane structure filled with FR4.

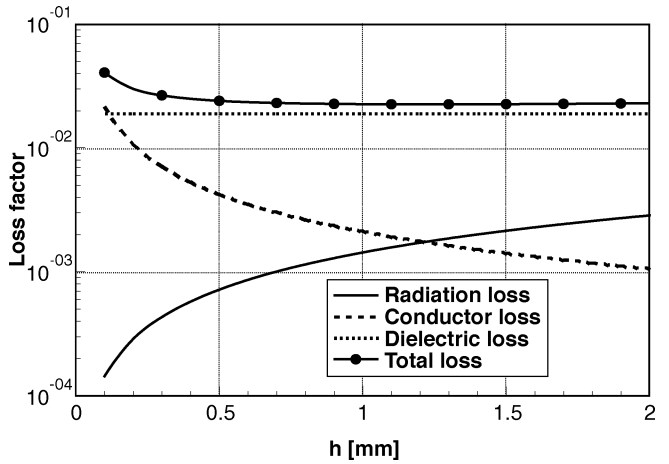

Fig. 3. Loss factors versus substrate thickness for a 16 cm $\times$ 10 cm power-ground plane structure filled with FR4 at the TM_{02} mode resonance.

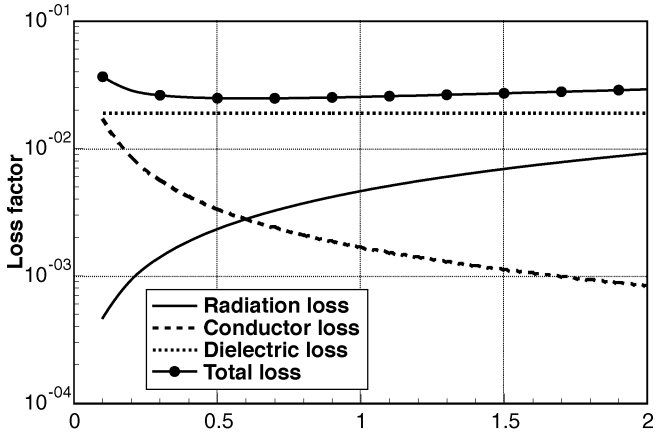

Fig. 4. Loss factors versus substrate thickness for a 16 cm $\times$ 10 cm power-ground plane structure filled with FR4 at the TM_{02} mode resonance.

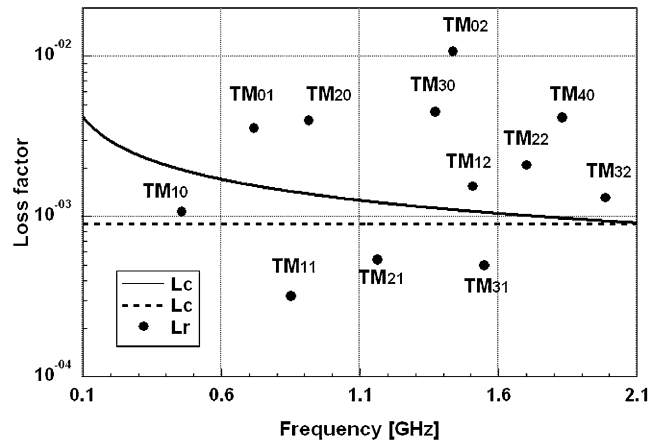

Fig. 5. Loss factors for a $22 \times 14 \times 0.157\,48$ cm^3 power-ground plane structure filled with Rogers RT/duroid 5880.

The conductor loss decreases inversely proportional to the square root of frequency, and is in the range from 5.657×10^{-3} to1.415×10^{-3}. The radiation loss factor varies from 5.819×10^{-3} to 1.366×10^{-4} depending on the resonant cavity mode order. In general, it is observed that radiation losses associated with modes with $m \neq 0$ and $n \neq 0$ (such as TM_{11}, TM_{21} and TM_{12} modes) are much smaller than that of other modes (such as TM_{01}, TM_{20}, TM_{30} and TM_{02} modes) with the exception of TM_{10} mode. For TM_{02} mode, the radiation loss factor goes as high as 5.819×10^{-3}. For this mode, the radiation loss must be considered in the modeling.

The three loss mechanisms are then investigated as a function of substrate thickness. Figs. 3 and 4 show the loss factors of TM_{20} and TM_{02} modes versus substrate thickness at the resonant frequencies. Again, the dielectric loss is independent of substrate thickness and modes. The conductor loss decreases (inversely proportional to h, as shown in (6) and (10)) when the substrate becomes thicker for both TM_{20} and TM_{02} modes. As the substrate thickness increases, the magnitude of the equivalent edge magnetic current, which is equivalent to edge voltage, as shown in [6], increases and, hence, more power is radiated into the free space. As a result, the radiation loss increases correspondingly. In fact, (20) shows that the stored energy is proportional to substrate thickness, h. According to Appendix A, spherical electric far-field components are also proportional to substrate thickness and, hence, the radiated power is proportional to h^2, as shown in (21). The radiation quality factor is therefore inversely proportional to substrate thickness and, consequently, the radiation loss factor is proportional to substrate thickness.

Fig. 3 shows the crossover point of radiation loss and conductor loss for the TM_{20} mode is around $h = 1.2$ mm. Similarly, Fig. 4 shows the crossover point for the TM_{02} is around $h = 0.6$ mm. For thin substrates, radiation loss is negligible compared to the dominant dielectric loss or even negligible compared to the conductor loss. However, for thick substrate, the radiation loss has to be taken into consideration.

The second example considered here is a low-dielectric-loss high frequency material, Rogers RT/duroid 5880. The board size is 22 cm $\times$ 14 cm. The substrate is 0.157 48 cm (62 mil) thick with a dielectric constant of 2.2 and a loss tangent of 0.0009. Fig. 5 shows a plot of the three loss factors as a function of frequency. In this case, the dielectric loss is very low, and, hence,

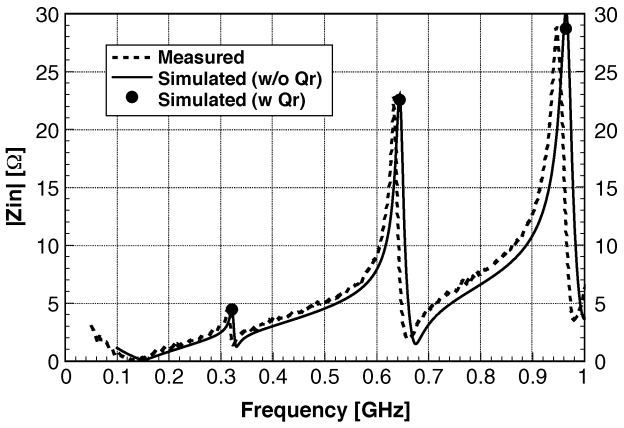

Fig. 6. Magnitude of input impedance of a 22.86 × 15.24 × 0.1588 cm^3 power-ground plane structure filled with FR4.

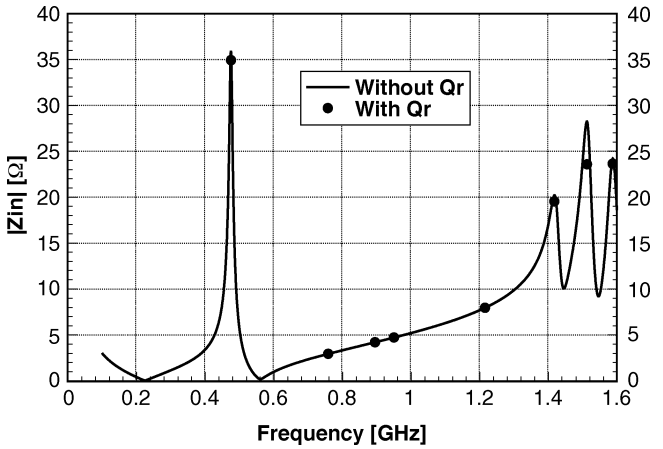

Fig. 7. Magnitude of input impedance of a $16 \times 10 \times 0.127$ cm^3 power-ground plane structure filled with FR4.

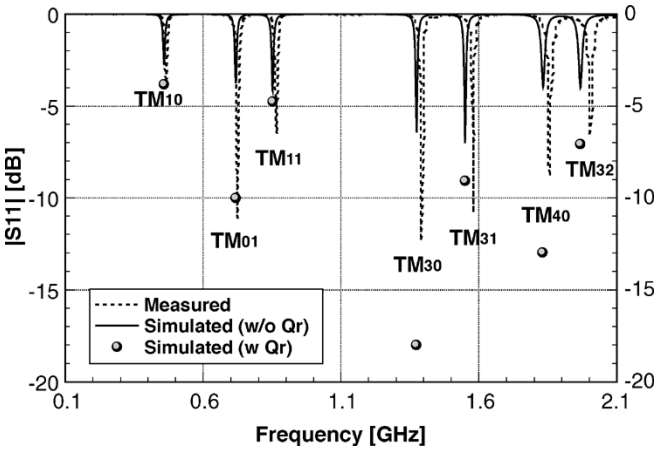

Fig. 8. Reflection coefficients for a 22 × 14 × 0.157 48 cm^3 power-ground plane structure filled with Rogers RT/duroid 5880.

the radiation loss and conductor loss become dominant factors. In addition, due to the thick substrate, the radiation loss can be much larger than the conductor loss at several resonant frequencies. For example, at the TM_{02} resonance, the radiation loss factor is greater than 0.01, which is far more important than both conductor loss factor and dielectric loss factor. Therefore, radiation loss must be considered for input impedance calculation. It is also observed that the radiation loss of modes with $m \neq 0$ and $n \neq 0$ is much less than that of other modes with either $m = 0$ or $n = 0$, except for TM_{10} mode.

Based on the above discussion, one can conclude that the radiation loss is proportional to the substrate thickness and closely related to the cavity mode order, while the conductor loss is inversely proportional to the substrate thickness. For high dielectric loss substrates, the dielectric loss is dominant. If the substrate is thin, the radiation loss can be neglected. However, when the substrate is thick (on the order of 1 mm), the radiation loss should be considered for accurate impedance calculation. For low dielectric loss substrates, the radiation loss and the conductor loss can be dominant.

B. Input Impedance

Once the quality factors are obtained, the effective wavenumber can be calculated from (4) and (5). Substituting the effective wavenumber into (14) yields the input impedance of a rectangular power-return structure. To validate our model, a FR4 board with a length of 22.86 cm and a width of 15.24 cm is studied. The substrate thickness is 0.1588 cm and relative dielectric constant is 4.1. The via locates at $x_0 = 9.65$ cm and $y_0 = 7.67$ cm. The radius of via is 0.035 cm. The input impedance is calculated with or without considering the radiation loss. The results are compared with the measured data in [20], as shown in Fig. 6. Due to the excitation position, only three modes, TM_{10}, TM_{20} and TM_{02} are excited within the frequency range. The predicted resonant frequencies are slightly different from the measured results, which is due to the assumption that the dielectric constant is frequency independent as well as the simplified edge extension model. The first two modes do not radiate much and, hence, the simulated data agree with the measured data very well, even without considering the radiation loss. For the third mode, neglecting the radiation loss introduces a 4.90% error in impedance prediction. With the radiation loss consideration, the error reduces to 0.35%.

The input impedance of the FR4 board, which was described in Fig. 2, is also studied. The magnitude of input impedance is shown in Fig. 7. Only four modes are excited within the simulated frequency range due to the excitation position. Since the dominant dielectric loss is very strong, the radiation loss can be neglected for most of the modes, except for TM_{02} mode. For TM_{02} mode, neglecting the radiation loss can cause about 20% error in the input impedance estimation. This can be explained by comparing the loss factors of both dielectric loss and radiation loss for the TM_{02} in Fig. 2. As shown in the figure, the radiation loss factor is a third of the dielectric loss factor. Therefore, it contributes significantly to the input impedance estimation.

Next, the RT/duroid board, which has a low dielectric loss is investigated. The via is located at $\mathrm{x}_0 = 5.5\,\mathrm{cm}$ and $\mathrm{y}_0 = 3.5\,\mathrm{cm}$. The reflection coefficient of the RT/duroid board is studied numerically and experimentally. The magnitude of reflection coefficient is shown in Fig. 8. At this via position, only seven modes are excited in a frequency range from 100 MHz to 2.1 GHz. As shown in the figure, without considering the radiation loss, the reflection coefficients are overestimated. This error could be significant depending on the operating modes, such as the second

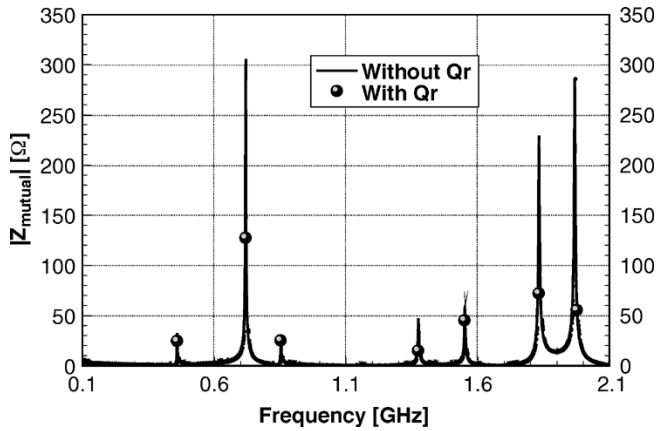

Fig. 9. Mutual impedance between point $x_0 = 5.5$ cm, $y_0 = 3.5$ cm and point $x_1 = 10.5$ cm, $y_1 = 12.5$ cm on a $22 \times 14 \times 0.15748$ cm^3 power-ground plane structure filled with Rogers RT/duroid 5880.

mode shown in the figure. When the radiation loss is considered at resonance frequencies, a better agreement can be observed. In particular, the first two modes match the measured data closely.

The figure also shows that the predicted resonance frequencies are lower than the measured resonance frequencies, especially at the high-frequency end. It is due to the approximation of fringing field compensation. The fringing field consideration also affects the estimation of reflection coefficients at the resonant frequencies. Furthermore, the assumption that the dielectric constant is independent on the frequency can also be one of the reasons responsible to the deviation. Currently, we are developing mode-dependent model to approximate the fringing effect and investigating the application of impedance boundary condition to improve the accuracy of input impedance estimation at high frequencies.

Fig. 9 shows the mutual impedance between a via at ($x_0 = 5.5$ cm, $y_0 = 3.5$ cm) and the other via at ($x_1 = 10.5$ cm, $y_1 = 12.5$ cm). As shown in the figure, without considering the radiation loss, the magnitudes of mutual impedance are overestimated. This error could be significant depending on the operating modes.

V. Conclusion

The radiation effect on via coupling in a rectangular power-return plane was studied. The radiation loss quality factor was investigated and compared to the dielectric loss and conductor loss quality factors. Numerical and experimental investigations were performed to demonstrate the radiation effects on via-to-substrate coupling for both high-dielectric-loss and low-dielectric-loss substrates. Theoretical analysis showed that the conductor loss is inversely proportional to the substrate thickness and the radiation loss is proportional to the substrate thickness. It was observed that without considering the radiation loss, the cavity model input impedance calculation can exhibit significant errors for low-dielectric-loss PCBs. For high-dielectric-loss PCBs, the dielectric loss is dominant. Hence, for thin substrates, the radiation loss is negligible. For thick substrates (substrate thickness on the order of 1 mm), the radiation loss, however, may become comparable to the dielectric loss and, hence, radiation effects must be considered in order to accurately predict the coupled noise. Results also show that the modes with $m \neq 0$ and $n \neq 0$ generally exhibited lower radiation loss than that of the modes with either $m = 0$ or $n = 0$.

Appendix
Evaluation of Radiated Power From Power-Return Planes

For completeness, the equations for the radiation power calculation are listed. They are developed in [6].

The far field from the power-return plane radiation can be described by

$$\vec{E} = A_{mn} h \frac{e^{-jk_0 r}}{4\pi r} (\vec{P}_L G_L S_L - \vec{P}_W G_W S_W) \tag{A1}$$

where

$$\vec{P}_L = \sin\varphi\hat{\varphi} + \cos\theta\cos\varphi\hat{\varphi}, \tag{A2}$$

$$\vec{P}_W = -\cos\varphi\hat{\varphi} + \cos\theta\sin\varphi\hat{\varphi}, \tag{A3}$$

$$S_L = \frac{jk_0 k_\xi}{\left(\frac{m\pi}{l_e}\right)^2 - k_\xi^2} G_W, \tag{A4}$$

$$S_W = \frac{jk_0 k_\eta}{\left(\frac{n\pi}{w_e}\right)^2 - k_\eta^2} G_L, \tag{A5}$$

$$G_L = 1 - (-1)^n e^{jk_\eta w_e}, \tag{A6}$$

$$G_W = 1 - (-1)^m e^{jk_\xi l_e} \tag{A7}$$

and

$$\begin{Bmatrix} k_\xi \\ k_\eta \end{Bmatrix} = k_0 \sin\theta \begin{Bmatrix} \cos\varphi \\ \sin\varphi \end{Bmatrix}. \tag{A8}$$

References

[1] G. T. Lei, R. W. Techentin, and B. K. Gilbert, "High-frequency characterization of power/ground-plane structures," *IEEE Trans. Microw. Theory Tech.*, vol. 47, no. 5, pp. 562–569, May 1999.

[2] J. C. Parker Jr., "Via coupling within parallel rectangular planes," *IEEE Trans. Electromagn. Compat.*, vol. 39, no. 1, pp. 17–23, Feb. 1997.

[3] M. Xu and T. H. Hubing, "The development of a closed-form expression for the input impedance of power-return plane structures," *IEEE Trans. Electromagn. Compat.*, vol. 45, no. 3, pp. 478–485, Aug. 2003.

[4] J. G. Yook, V. Chandramouli, L. P. B. Katehi, K. A. Sakallah, T. R. Arabi, and T. A. Schreyer, "Computation of switching noise in printed circuit boards," *IEEE Trans. Compon. Packag., Manuf. Technol. A*, vol. 20, no. 1, pp. 64–75, Mar. 1997.

[5] H. Liaw and H. Merkelo, "Simulation and modeling of mode conversion at vias in multilayer interconnects," in *Proc. IEEE 45th Electronic Components and Technology Conf.*, 1995, pp. 361–367.

[6] M. Leone, "The radiation of a rectangular power-bus structure at multiple cavity-mode resonances," *IEEE Trans. Electromagn. Compat.*, vol. 45, no. 3, pp. 486–492, Aug. 2003.

[7] W. Shi and J. Fang, "New efficient method of modeling electronics packages with layered power/ground planes," *IEEE Trans. Adv. Packag.*, vol. 25, no. 3, pp. 417–423, Aug. 2002.

[8] R. L. Chen and J. Chen, "Radiation effects on via coupling in power-return plane structures," *Microw. Opt. Technol. Lett.*, pp. 117–119, Apr. 20, 2004.

[9] T. Itoh, "Spectral domain immitance approach for dispersion characteristics of generalized printed transmission lines," *IEEE Trans. Microw. Theory Tech.*, vol. 28, no. 7, pp. 410–413, Jul. 1980.

[10] E. F. Kuester, R. T. Hohnk, and D. C. Chang, "The thin-substrate approximation for reflection from the end of a slab-loaded parallel-plate waveguide with application to microstrip patch antennas," *IEEE Trans. Antennas Propag.*, vol. 30, no. 5, pp. 910–917, Sept. 1982.
[11] Y. T. Lo, D. Solomon, and W. F. Richards, "Theory and experiment on microstrip antennas," *IEEE Trans. Antennas Propag.*, vol. 27, no. 2, pp. 137–145, Mar. 1979.
[12] E. O. Hammerstad, "Equations for microstrip circuit design," in *Proc. 5th Eur. Microwave Conf.*, 1975, pp. 268–272.
[13] M. Kara, "Formulas for the computation of the physical properties of rectangular microstrip antenna elements with various substrate thickness," *Microw. Opt. Technol. Lett.*, vol. 12, pp. 234–239, 1996.
[14] D. R. Jackson, "Analysis techniques for microstrip antennas," presented at the IEEE Antennas and Propagation Society Int. Symp. (Part II of Short Course on the Analysis and Design of Microstrip Antennas and Arrays), Chicago, IL, Jul. 1992.
[15] T. Okoshi, *Planar Circuits for Microwaves and Lightwaves*. New York: Springer-Verlag, 1985.
[16] D. M. Pozar, "Improved computational efficiency for the moment method solution for printed dipoles and patches," *Electromagnetics*, vol. 13, pp. 299–309, 1983.
[17] G. T. Lei, R. W. Techentin, P. R. Hayes, D. J. Schwab, and B. K. Gilbert, "Wave model solution to the ground/power plane noise problem," *IEEE Trans. Instrum. Meas.*, vol. 44, no. 2, pp. 300–303, Apr. 1995.
[18] J. R. James, P. S. Hall, and C. Wood, *Microstrip Antennas: Theory and Design*. Stevenage, U.K.: Peregrinus, 1981.
[19] C. A. Balanis, *Antenna Theory: Analysis and Design*. New York: Wiley, 1996.
[20] W. Shi, "Modeling and simulation of electronics packages for signal integrity and electromagnetic compatibility," Ph.D. dissertation, Dept. Elect. Comput. Eng., Binghamton Univ., Binghamton, NY, 1999.

Richard L. Chen (S'00–M'04) received the B.S. degree in physics and the M.S.E.E. degree from Southeast University, Nanjing, China, in 1992 and 1995, respectively, and the Ph.D. degree in electrical engineering from the University of Houston, Houston, TX, in 2003.

He is a Postdoctoral Research Associate in the Department of Electrical and Computer Engineering, University of Houston. His research interests include microstrip antennas and arrays, nano-scale frequency selective surfaces, and signal integrity.

Dr. Chen is a Member of the IEEE Antennas and Propagation and IEEE Microwave Theory and Techniques Societies. He received the Best Presentation Award at ION GPS/GNSS 2003, held in Portland, OR.

Ji Chen (S'93–M'98) received the Bachelor degree from Huazhong University of Science and Technology, Huazhong, China, in 1989, the Masters degree from McMaster University, Hamilton, ON, Canada, in 1994, and the Ph.D. degree from the University of Illinois at Urbana-Champaign in 1998, all in electrical engineering.

He is currently an Assistant Professor in the Department of Electrical and Computer Engineering, University of Houston, Houston, TX. Before he joined the University of Houston, he was a Staff Engineer at the Motorola Personal Communication Research Laboratories, Chicago, IL, from 1998 to 2001.

Dr. Chen received a Motorola Engineering Award in 2000.

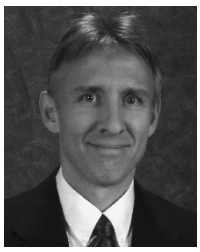

Todd H. Hubing (S'82–M'82–SM'93) received the B.S.E.E. degree from the Massachusetts Institute of Technology, Cambridge, in 1980, the M.S.E.E. degree from Purdue University, West Lafayette, IN, in 1982, and the Ph.D. degree in electrical engineering from North Carolina State University, Raleigh, in 1988.

From 1982 to 1989, he was with the Electromagnetic Compatibility Laboratory, IBM Communications Products Division, Research Triangle Park, NC. In 1989, he decided that he wanted to spend less time fixing EMC problems and more time trying to understand them, so he left IBM to join the faculty at the University of Missouri, Rolla (UMR). He is currently a Professor of Electrical and Computer Engineering and part of a team of faculty and students at UMR that are working to solve a wide range of EMC problems affecting the electronics industry. He teaches the "Grounding and Shielding" and "High-Speed Digital Design" courses at UMR.

Prof. Hubing has received several awards for teaching and faculty excellence. He was an Associate Editor of the IEEE TRANSACTIONS ON ELECTROMAGNETIC COMPATIBILITY, the *IEEE Electromagnetic Compatibility Society Newsletter*, and the *Journal of the Applied Computational Electromagnetics Society*. He was the 2002–2003 President of the IEEE Electromagnetic Compatibility Society and continues to serve on the Board of Directors.

Weimin Shi (M'92–SM'00) received the B.S. and M.S. degrees in radio engineering from Southeast University, Nanjing, China, in 1987 and 1990, respectively, and the Ph.D. degree in electrical engineering from the State University of New York, Binghamton, in 1999.

He joined Intel Corporation at the end of 1999 and is currently with the Mobile Platform Group, Beaverton, OR as a Staff engineer. His research interests include the modeling of signal integrity, packaging power delivery, electromagnetic compatibility/interference, and electrostatic discharge phenomena in high-speed electronic systems. From 1990 to 1995, he was with Nanjing University of Aeronautics and Astronautics, where he conducted research on antennas, EM wave scattering, and microwave/millimeter-wave systems. From 1995 to 1996, he was with the Department of Electronic Engineering, City University of Hong Kong, as a Research Assistant, performing research on W-band millimeter-wave groove-guide systems. From 1996 to 1999, he was with the State University of New York, Binghamton, as a Research Assistant, concentrating on modeling and simulation of the electrical performance of packages. In 1999, he was briefly with Cornell University as a Research Associate, conducting research on high-speed electronic packaging.